Available online at www.sciencedirect.com
SCIENCE DIRECT
Dyes and Pigments 72 (2007) 163–177
DYES and PIGMENTS
www.elsevier.com/locate/dyepig

The photochromic effect of bismuth vanadate pigments: Investigations on the photochromic mechanism

Andreas Tücks, Horst P. Beck*

Institute of Inorganic and Analytical Chemistry and Radiochemistry, Saarland University, P.O. Box 15 11 50, D-66041 Saarbrücken, Germany

Received 23 June 2005; accepted 19 August 2005
Available online 28 November 2005

Abstract

We report on investigations of the photochromic effect of $BiVO_4$ pigments focussing on pigment powder samples. Results are compared to those of the corresponding pigment coatings, and we discuss the differences and similarities concerning photochromism. Besides impurity levels of Fe and Pb, the specific surface area of pigment particles as well as interactions between the particles and their surroundings turn out to be important factors that determine the degree of color change. The outcomes of illumination experiments in different atmospheres and powder EPR spectroscopy suggest formation of V^{IV} and photochemical red-ox disproportionation of Fe^{III} to be the central processes in the so-called V-type and Fe-type mechanisms, respectively, but details of a further mechanism (Pb-type) are not yet well understood.

Keywords: $BiVO_4$; Pigment powders; Photochromism; Colorimetry; Reflectance spectroscopy; Electron spin resonance spectroscopy

1. Introduction

The pigment industry spends much effort on finding new products that meet the needs of the market, but further improvements of existing and already commercialized pigments play an important role as well. Among the properties of interest are color properties and, among these, lightfastness is a fundamental one. In contrast to the latter, the term photochromism implies the reversibility of color change and has been observed for a variety of inorganic compounds (e.g., V_2O_5 [1], MoO_3 [2], WO_3 [3,4], perovskites [5–7], $PbMoO_4$ [8], photochromic glasses [9,10]). Changes in optical properties due to illumination are desired for materials that find application in optical information storage [11,12], but the opposite is true in the case of pigments. $BiVO_4$ is one of the more common pigments that may exhibit photochromic effects depending on the method of preparation and after-treatment.

Our results of foregoing investigations on pigment coatings, which were reported elsewhere [13], are both important and helpful for the discussion presented in the subsequent sections. Most notably is the finding that small amounts of impurity phases, which may form depending on the synthesis conditions, do not significantly affect the extent of photochromism.[1] On the other hand, impurities on an atomic scale (trace impurities and dopants) can cause drastic color changes on illumination with artificial light or natural daylight. ICP-MS was applied to determine the doping concentrations of more than 20 elements. The results point to the central role of Fe and Pb in different photochromic mechanisms. To confirm this assumption, $BiVO_4$ was doped with a variety of elements, but only doping with Fe and Pb yielded highly photochromic pigments. The situation becomes more complicated due to the fact that pigments synthesized by solid-state reaction turned out to exhibit strong photochromism despite low or medium impurity levels. Therefore, other parameters must be taken into account to explain the varying lightfastness of different pigments. This point will be discussed in detail in Section 3. Finally, the method of quantifying photochromic effects needs

* Corresponding author. Tel.: +49 681 302 2421; fax: +49 681 302 4233.
E-mail address: hp.beck@mx.uni-saarland.de (H.P. Beck).

[1] All samples were analyzed not only by X-ray powder diffraction but also by infra-red spectroscopy to detect amorphous phases like, e.g., V_2O_5.

0143-7208/$ - see front matter © 2005 Elsevier Ltd. All rights reserved.
doi:10.1016/j.dyepig.2005.08.027

some explanation because it involves colorimetry, which provides the means to quantitatively describe colors in a systematic and objective way. Different color spaces (vector spaces from a mathematical standpoint) exist, but all of them share the property that three numbers (color co-ordinates) are required for each color perceivable by the human eye. We have chosen the CIELAB color space because it is widely applied in industrial test methods and suitable to describe colors and, more important, color differences (ΔE_{ab}*-value). For more details see Ref. [13] and the literature cited therein.

Color co-ordinates, and thus color differences, are calculated from reflectance spectra of the samples in question, but the spectra themselves can also give valuable information to distinguish different photochromic mechanisms (PCM). The difference of two such spectra obtained from an illuminated and non-illuminated sample, the ''difference reflectance spectrum'' (DRS), has turned out to be a suitable indicator for this purpose. We have shown that according to DRS of a large set of pigment coatings, at least three kinds of mechanisms (Fe-type, Pb-type and V-type) can be distinguished [13].

In the following sections, we focus on powder samples and their properties including lightfastness, specific surface areas as well as interactions between pigment particles and the surrounding medium. Furthermore, electron paramagnetic resonance studies provide an understanding of mechanistic details on an atomic scale.

2. Experimental

2.1. Pigment synthesis and after-treatment

Pigments were synthesized by either wet-chemical precipitation or solid-state reaction using different combinations of educts. A detailed description can be found in Ref. [13]. Table 1 only describes the thermal and mechanical after-treatment of the pigments. Both directly affect the particles' surface properties, which will be important in the subsequent discussion (see Section 3).

2.2. Illumination experiments

Pigment powders were gently pressed into disc-shaped sample holders made from brass (inner diameter, 26 mm; depth, 2 mm). All samples were illuminated for a period of 90 min with a 1000 W tungsten halogen lamp (distance, 50 cm from sample surface) and kept in the dark for 30 min before reflectivity measurements were carried out. To illuminate powder samples in atmospheres other than air, sample holders were placed in aluminum cells coated with black photoresist and sealed with ordinary glass windows (thickness, 4.5 mm; UV cut-off at approx. 350 nm). Prior to light exposure, one of the following atmospheres was established inside the corresponding cell: air (reference), oxygen, air enriched with ethanol, and vacuum.

Table 1
Standard thermal and mechanical treatment of pigment raw-products (dried at 130 °C)

Method	Annealing	Ball-milling
Wet-chemical synthesis (precipitation)	<500 °C	None
	2 h at 500 °C	1 h/none[a]
	2 h at 500 °C + 0.5 h at 620 °C	1.5 h
	3 × 10 h at 650 °C	12 h
Solid-state reaction	2 × 10 h at 650 °C	12 h
	3 × 10 h at 650 °C	12 h

[a] Illumination of powders was carried out with both kinds of samples.

2.3. UV–Vis spectroscopy

Diffuse reflectance spectra were recorded on a double-beam UV–Vis-NIR spectrometer *Lambda 19* (Perkin–Elmer) equipped with an integrating sphere RSA-PE-19 (Labsphere) in 8/d geometry without inclusion of gloss. In order to rule out any contamination of the integrating sphere, the sample holder was sealed with a quartz window (thickness, 1 mm). For data evaluation, three spectra of each sample were averaged and converted to absolute reflectivity values. Due to the preparation method, the precision of ΔE_{ab}*-values is worse for powder samples than for coated test-sheets, and differences of approximately 1 unit can be considered to be significant (approx. 0.4 units for coatings).

2.4. Electron paramagnetic resonance spectroscopy

EPR spectra at X-band frequencies were recorded on an ESP300 spectrometer (Bruker) equipped with a continuous helium flow cryostat ESR900 (Oxford Instruments). Measurements were carried out at 20 K with modulation amplitudes of 0.5 or 1 mT and a modulation frequency of 100 kHz. Generally, pigments were ground in an agate mortar to a fine powder and filled into EPR quartz tubes (Wilmad). Instead of attempting to quantitatively determine the spin concentration of each sample, signal intensities of ex situ illuminated and non-illuminated samples of a given pigment were compared. To minimize systematic errors, approximately the same amounts of powder were weighed (less than 4% mass difference) and the corresponding spectra recorded immediately one after another to avoid instrumental drift. Finally, all spectra were mass-normalized.

2.5. Scanning electron microscopy

Scanning electron micrographs were taken on an SEM 840A (Jeol) equipped with a tungsten hairpin filament.

2.6. Surface measurements

Specific surface areas were determined by means of the single-point BET method on a *Sorpty 1750* (Fisons Instruments). All samples were dried in vacuum at 200 °C for 12 h before measurement. All results given in Section 3 are mean values of three or four individual measurements.

2.7. Determination of crystallite sizes and microstrain

Microstructural parameters [14] were calculated from powder diffraction patterns using the program *FormFit*, which is part of the software package *Erlray* (Copyright © 2002, R. Haberkorn [15]). Instrumental broadening was empirically determined with a suitable reference substance (LaB_6).

2.8. Quantification of photochromism

In Ref. [13] we discussed the methods to quantify the photochromic effect and emphasized the importance and usefulness of colorimetry [16]. Regarding the latter, the outlined procedure is applicable to powder samples as well, but comparisons between color properties of lacquers and powders in terms of hue h_{ab}*, chroma C_{ab}*, and lightness L* are not of interest. Both types of samples differ considerably in properties like pigment concentration, degree of agglomeration and refractive index of the surrounding medium. In the end, the color properties of the finished products (i.e., coatings or colored plastics) are decisive. Nevertheless, colorimetric data can still be applied to visualize and discuss the influence of thermal/mechanical treatment within a series of powder samples, and ΔE_{ab}*-values (defined by $\Delta E^*_{ab} = \sqrt{\Delta L^{*2} + \Delta a^{*2} + \Delta b^{*2}}$, where a* and b* constitute the x- and y-axes of the CIELAB color space, respectively) provide a well-defined benchmark to characterize the extent of photochromism.

3. Results and discussion

3.1. Illumination of powder samples

The everyday handling of photochromic pigments has shown that different sample types, i.e., powders or lacquers, of the same pigment can vary significantly in lightfastness. Whereas the pigment industry predominantly focuses on the lightfastness of lacquers, which can be considered as final products and relevant to customers, studies of powder samples will yield additional information with regard to mechanistic details of photochromism. Table 2 gives a comparison between both kinds of samples for a selection of compounds.

It has already been pointed out that color properties of lacquers and powders should not be directly compared. Therefore, it is appropriate to pick out one or several pigments as reference samples, and these pigments can then be used for further comparisons within both groups of sample types. BV-149, BV-Sb/0.1, and BV-Mo/0.2, which exhibit almost the same ΔE_{ab}* in both cases, are suitable candidates.

Compared to pigment coatings, powder samples span a wider range of ΔE_{ab}*-values. No color change is observable for Ca- and Sr-doped compounds, but ΔE_{ab}*-values as large as 40–50 can be achieved by doping with 0.5 mol-% Pb. Pigments with increased levels of Fe (e.g., BV-107, BV-134, Fe-doped compounds) show remarkable drops in ΔE_{ab}* if applied in lacquers, and the same holds true for Pb-doped samples as well. This is one of the several indications for interactions between pigment particles and their surroundings.

Table 2
Comparison between ΔE_{ab}*-values of powder samples (P) and the corresponding pigment coatings (C)

Sample	After-treatment	ΔE_{ab}* (P)	ΔE_{ab}* (C)	Sample[a,b]	ΔE_{ab}* (P)	ΔE_{ab}* (C)
BV-107	2 h 500 °C	9.7	5.3	BV-Ca/5	0.2	1.1
BV-109	2 h 500 °C	2.1	2.5	BV-Sr/5	0.2	1.4
BV-116	2 h 500 °C	3.0	1.7	BV-Pb/0.1	24.1	7.1
	2 h 750 °C[c]	1.8	3.4	BV-Sb/0.1	2.7	2.6
BV-119	2 h 500 °C	1.4	1.4	BV-Cr/0.1	0.9	0.8
BV-126	2 h 500 °C	3.2	1.3	BV-Mo/0.2	2.9	2.9
BV-134	2 h 500 °C	12.8	4.5	BV-W/0.2	2.5	3.0
BV-137	3 × 10 h 650 °C	1.2	5.6	BV-Mn/0.1	3.0	3.3
BV-138	2 h 500 °C	0.7	2.6	BV-Fe/0.1	24.5	6.3
BV-139	2 h 500 °C	0.6	3.0	BV-Fe/0.2	23.4	7.7
BV-140	2 h 500 °C	3.5	0.9	BV-Co/0.1	1.5	3.5
	3 × 10 h 650 °C	0.9	3.0	BV-Ni/0.1	3.1	2.4
BV-141	2 h 500 °C	2.8	2.2	BV-Cu/0.1	1.2	2.5
	3 × 10 h 650 °C	1.1	2.8	BV-Ag/0.1	7.7	2.6
BV-147	3 × 10 h 650 °C	1.5	5.4	BV-Zn/2	6.0	2.6
BV-149	2 h 500 °C + 0.5 h 620 °C	2.8	2.6	BV-Ce/0.1	0.9	1.4
				BV-Eu/0.1	3.6	2.5

[a] Sample names of doped pigments include the nominal doping concentration (mol-%).
[b] Except for BV-Ag/0.1 and BV-Zn/2 (2 h 500 °C) all doped pigments were annealed at 500 °C for 2 h and additionally at 620 °C for 30 min. For details on mechanical treatment see Table 1.
[c] 6 h ball-milling.

BV-138, exhibiting the lowest impurity levels of all pigments (especially with regard to Fe), yields an average and somewhat disappointing ΔE_{ab}* of 2.6 as coating but only 0.7 units as powder. Another striking point is the tendency of decreasing lightfastness with increasing temperature of thermal treatment. The latter requires extended periods of ball-milling, predominantly for dispersibility reasons. The results listed in Table 2 clearly show the opposite behavior for powder samples (e.g., consider BV-116, BV-140, BV-141). Obviously, more information about surface properties is needed because the extent of interactions with the surrounding medium (lacquer or air) strongly depends on the surface boundary. Before discussing the results of surface measurements as well as scanning electron micrographs, the DRS of selected powder samples are compared to those of pigment lacquers.

Fig. 1 shows DRS of BV-149, BV-Pb/0.1, and BV-Fe/0.1. In all cases, the same after-treatment was applied (annealing 2 h 500 °C + 0.5 h 620 °C, 1.5 h ball-milling). Again, the same spectral features (not intensities!) that we used to differentiate PCMs of pigment coatings [13] can be observed for powders. Minor differences arise due to the fact that pigment particles in powders are agglomerated and surrounded by air instead of baking finish. Fe-doped compounds exhibit a ''double-band structure'' between approx. 500 and 800 nm as well as slowly decreasing intensities towards higher wavelengths. Pb containing pigments only show single peaks that fall off sharply. In contrast, a series of undoped pigments, to which BV-149 belongs, differ from the latter group regarding the curve shape and maximum intensities (lower ΔE_{ab}*-values) of their DRS. With increasing

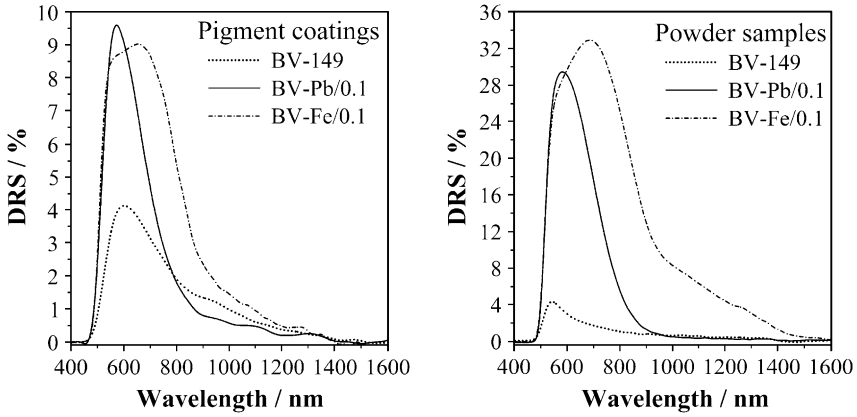

Fig. 1. DRS of BV-149, BV-Fe/0.1 and BV-Pb/0.1 for coatings (left) and powder samples (right).

wavelength, intensities decrease more slowly from the corresponding maximum value. As this set of criteria applies for both sample types, and the majority of pigments under study can be classified accordingly, we will label the three types of PCMs as Fe-type, Pb-type, and V-type.

Next, we will discuss the opposite trends of ΔE_{ab}*-values that are observed for powders and coatings with increasing temperature of annealing and the necessary change in mechanical treatment. Figs. 2 and 3 show a series of DRS for BV-134 (high levels of Fe), BV-149, BV-Fe/0.1, and BV-Pb/0.1. When measuring reflectance spectra of powder samples, ball-milling can be avoided by annealing the raw-products below approx. 550 °C.[2] Besides the standard procedures given in Section 2, selected pigments were heated to 300 and 400 °C for 2 h.

Inspecting the curves in Figs. 2 and 3, we can conclude that the maximum photochromic effect results if annealing is carried out at 500 °C. Some kind of ageing can be observed for BV-134 and BV-149 annealed at 300 °C, which is indicated by a crossing of reflectance spectra of the illuminated and non-illuminated sample, i.e., by partially negative DRS. Comparing BV-Fe/0.1 and BV-Pb/0.1, it is most noticeable that, while the general trend is obviously identical, only a small ΔE_{ab}*-value is obtained in the case of BV-Fe/0.1 heated to 300 °C. Passing the ''500 °C boundary'', drops in ΔE_{ab}* result, which are especially considerable if annealing conditions correspond to those used in our solid-state reactions. Here, the crucial point turns out to be the mechanical treatment of the samples in question. Compact powders consisting of hard grains require sufficient ball-milling for sample preparation. All DRS shown in Figs. 2 and 3 that are not marked by asterisks were derived from samples subjected to ball-milling according to Table 1. It is self-evident that this aspect deserves a closer look.

Generally, increasing annealing temperatures result in enhanced crystallite and grain growth (see Section 3.2), but another point, the incorporation of impurities or dopants into the crystal at appropriate lattice sites, should not be overlooked in the discussion. Considering the applied preparation method (wet-chemical precipitation), one must not expect all dopant elements (e.g., Fe or Pb) to occupy regular lattice sites of Bi or V in the raw-product of $BiVO_4$. In fact, the difference in lightfastness of BV-Fe/0.1 and BV-Pb/0.1 annealed at 300 °C can be explained on this basis. Resorting to ionic radii provided by Shannon and Prewitt [17], the radius of Fe^{III} (63 pm, c.n. 4, high-spin) is 27% larger than that of V^{V} (49.5 pm, c.n. 4). On the other hand, Pb^{II} (143 pm, c.n. 8) can easily adopt the Bi site (Bi^{III}: 131 pm, c.n. 8), the radius of the latter being smaller by only 8%. Therefore, higher temperatures are needed to make Fe occupy the V position [18] in the crystal lattice.[3] The location of impurities is of central importance for their influence on photochromic properties because wave functions and energies of defect states strongly depend on the immediate surroundings.

3.2. Surface properties and microstructure

Ball-milling directly affects the surface properties of pigments and yields powders with specific surface areas, A_{sp}, larger than that of the starting compounds. More intense interactions across the contact boundary between adjacent phases become possible. Increasing surface areas, which result from decreasing particle diameters (grain size), are usually accompanied by decreasing crystallite sizes as well. Due to mechanical forces acting on the grains, microstrain can also increase considerably. Overall, there are two main effects, heating and ball-milling, that determine the surface areas of the samples and act in opposite directions. This circumstance gives rise to a minimal value of A_{sp} under certain conditions. Table 3 shows a list of surface areas and microstructural parameters for five undoped pigments subjected to different thermal and mechanical after-treatments.

[2] In most cases, the preparation of pigment coatings requires ball-milling for dispersibility reasons even if the pigment in question is annealed at only 500 °C.

[3] Basically, the structure of $BiVO_4$, which is made up of Bi^{3+} ions and VO_4^{3-} tetrahedra packed in a Scheelite-type manner, offers enough space for Fe^{III} to occupy interstitial sites, but to our knowledge no information on that point is available up to now.

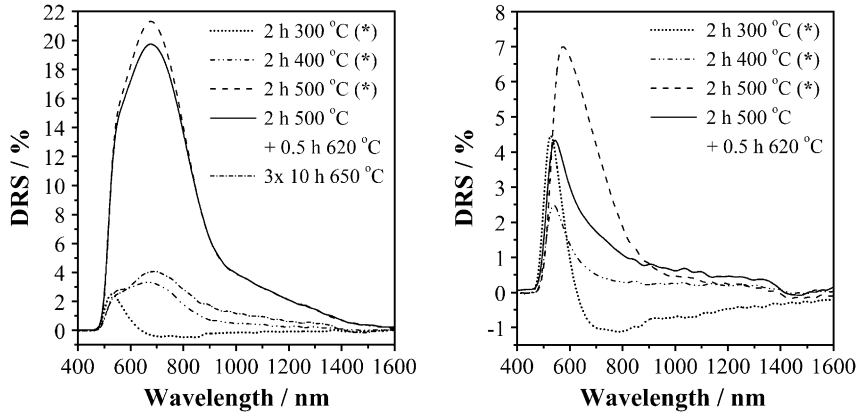

Fig. 2. DRS of BV-134 (left) and BV-149 (right) powder samples annealed at different temperatures (samples marked with an asterisk were not subjected to ball-milling but thoroughly ground in an agate mortar).

The lowest A_{sp} is generally found if pigments are annealed at 500 °C. In turn, maximal crystallite sizes L_{vol} as well as minimal microstrain ε_0 result at that temperature. Although the thermal treatment is more vigorous in these cases, the largest surface areas are observed for samples that are annealed according to solid-state reactions (3 × 10 h 650 °C), i.e., the ball-milling more than compensates for the thermally caused grain growth. The latter statement can be verified by scanning electron microscopy. Fig. 4 shows micrographs of BV-141 (2 h 500 °C, 1 h ball-milling; 3 × 10 h 650 °C, 12 h ball-milling) and BV-147 (solid-state reaction, 3 × 10 h 650 °C, 12 h ball-milling) at magnifications of 1:5000 and 1:20,000.

3.3. Illumination experiments in different atmospheres

To investigate the influence of the medium surrounding the pigment particles on the photochromic effect, illumination experiments with powder samples were carried out in different atmospheres. In most cases, commercially available pigments are coated with one or several layers of inorganic compounds that modify properties like dispersibility, chemical stability or lightfastness. As these ‘‘multi-phase systems’’ are less defined in regions where pigment and coating get into contact and, therefore, more difficult to study with respect to possible PCMs, only lacquers with uncoated pigments were prepared. This circumstance enables pigment–lacquer interactions to gain importance. For alkyd based baking finishes, such as those used in our study, the impact on the pigment particles is reductive in character and caused by hydroxyl groups that have not been quantitatively esterified. On the other hand, carboxylic groups can act as proton donors for charge compensation, depending on the type of reaction that takes place during illumination.

The bar charts in Fig. 5 show results for six different powder samples illuminated in air, pure oxygen, air enriched with ethanol, and vacuum. Regarding the effect of changing the atmosphere from air to reducing media, two groups can clearly be distinguished. We find considerably decreasing ΔE_{ab}*-values for the three examples on the left-hand side. However, the opposite is true for the remaining three samples (dark grey bar charts). The main difference between both groups is their specific surface area, which is significantly lower for BV-134 (2 h 500 °C), BV-Fe/0.1, and BV-Pb/0.1. BV-138 does not exactly fit into this scheme but contains much less impurities

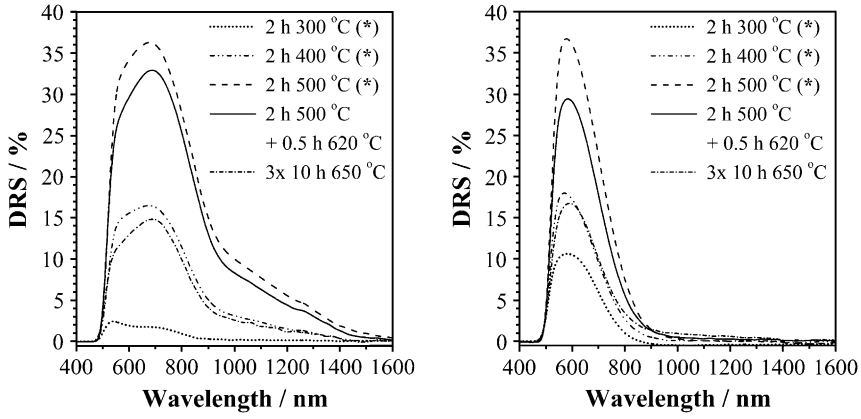

Fig. 3. DRS of BV-Fe/0.1 (left) and BV-Pb/0.1 (right) powder samples annealed at different temperatures (samples marked with an asterisk were not subjected to ball-milling but thoroughly ground in an agate mortar).

Table 3
Specific surface areas (A_{sp}) and microstructural parameters (L_{vol}, ε_0) of pigment samples

Sample	After-treatment	$A_{sp}/m^2\ g^{-1}$	L_{vol}/nm	ε_0/%
BV-134	2 h 400 °C	4.8	77 (1)	0.061 (2)
	2 h 500 °C, 1 h ball-milling	0.9	250 (7)	0.009 (1)
	3 × 10 h 650 °C, 12 h ball-milling	11.4	44 (2)	0.134 (3)
BV-138	2 h 500 °C, 1 h ball-milling	2.1	63 (1)	0.096 (3)
BV-140	2 h 500 °C, 1 h ball-milling	1.3	>300	0.010 (1)
	3 × 10 h 650 °C, 12 h ball-milling	8.3	56 (1)	0.109 (3)
BV-141	2 h 500 °C	0.8	>300	0.017 (1)
	2 h 500 °C, 1 h ball-milling	1.4	>300	0.002 (1)
	2 h 500 °C + 0.5 h 620 °C, 1 h ball-milling	2.3	145 (2)	0.050 (1)
	3 × 10 h 650 °C, 12 h ball-milling	8.0	57 (1)	0.104 (3)
BV-147	3 × 10 h 650 °C (ssr), 12 h ball-milling	5.4	80 (1)	0.082 (2)

than the former samples (e.g., BV-134: 46 ppm Fe, BV-138: 7 ppm Fe). It has been mentioned that the lightfastness of BV-138 in lacquers is worse than expected from the results of trace analysis. Illumination of powders in air/ethanol, which was chosen to "simulate" the reductive conditions in the applied baking finish, confirms this unexpected behavior and emphasizes the possibility that photochromism is not solely caused by increased impurity levels. The outcome of BET studies suggests BV-134 and BV-147 (both annealed for 3 × 10 h at 650 °C, 12 h ball-milling) to exhibit stronger interactions with the surrounding atmosphere due to their large surface area. Especially the comparison between both samples of BV-134 (different A_{sp}, same Fe levels) reveals important hints about the active PCM. With low surface areas, reductive media diminish the effect of Fe and yield lower ΔE_{ab}*-values. This, in turn, underlines the participation of Fe in higher oxidation states (e.g., Fe^{IV}) in the Fe-type PCM. The same applies to BV-Fe/0.1 and, in principle, to BV-Pb/0.1 as well. For the second sample of BV-134 (upper right bar chart), a different PCM can be expected because within the given row there is a steady increase in ΔE_{ab}*, i.e., photochromism is not partially reduced but enhanced.

For illumination experiments carried out in pure oxygen, results are more difficult to interpret. BV-147 is the only sample that shows a slightly increasing ΔE_{ab}*-value compared to illumination in air. All other pigments exhibit better lightfastness, which is especially true for BV-138. If we consider electron–hole pair formation as the starting point of the PCM, the lifetime of electron–hole pairs is an important parameter. Radiationless decay (thermal quenching) or fast relaxation via defect states between valence and conduction band reduce

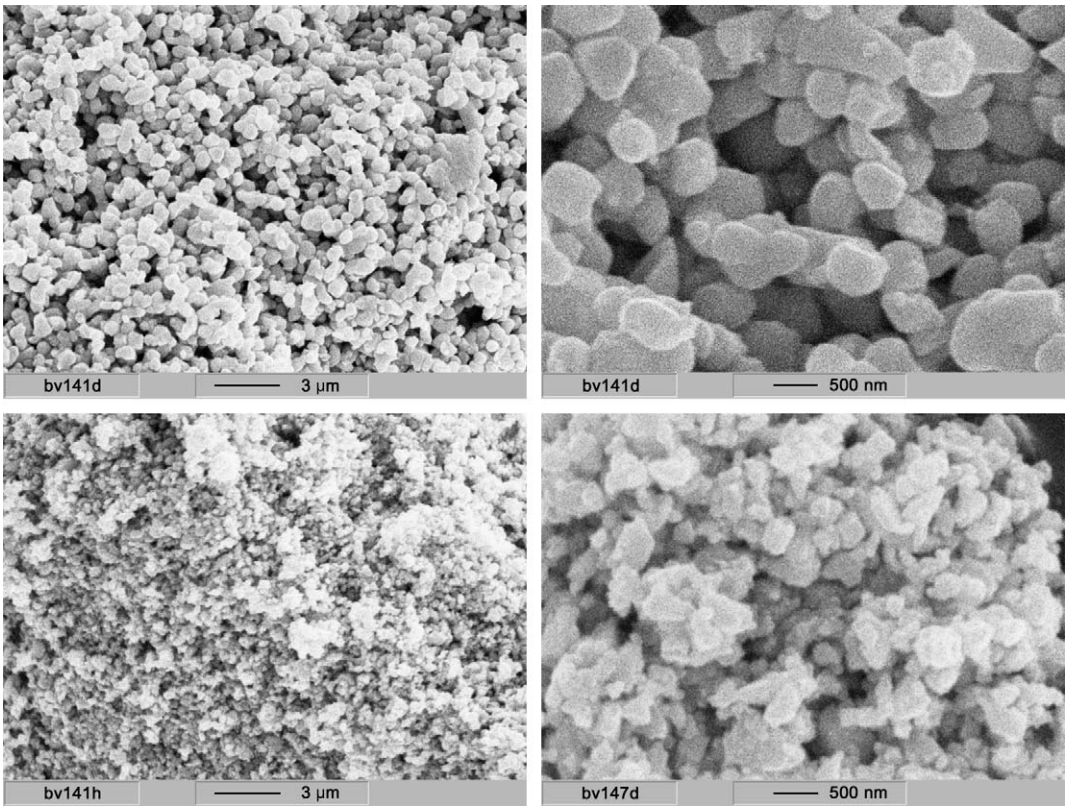

Fig. 4. Scanning electron micrographs of undoped $BiVO_4$ pigments subjected to different after-treatments (upper left and right: BV-141, 2 h 500 °C, 1 h ball-milling; lower left: BV-141, 3 × 10 h 650 °C, 12 h ball-milling; lower right: BV-147, 3 × 10 h 650 °C, solid-state reaction, 12 h ball-milling).

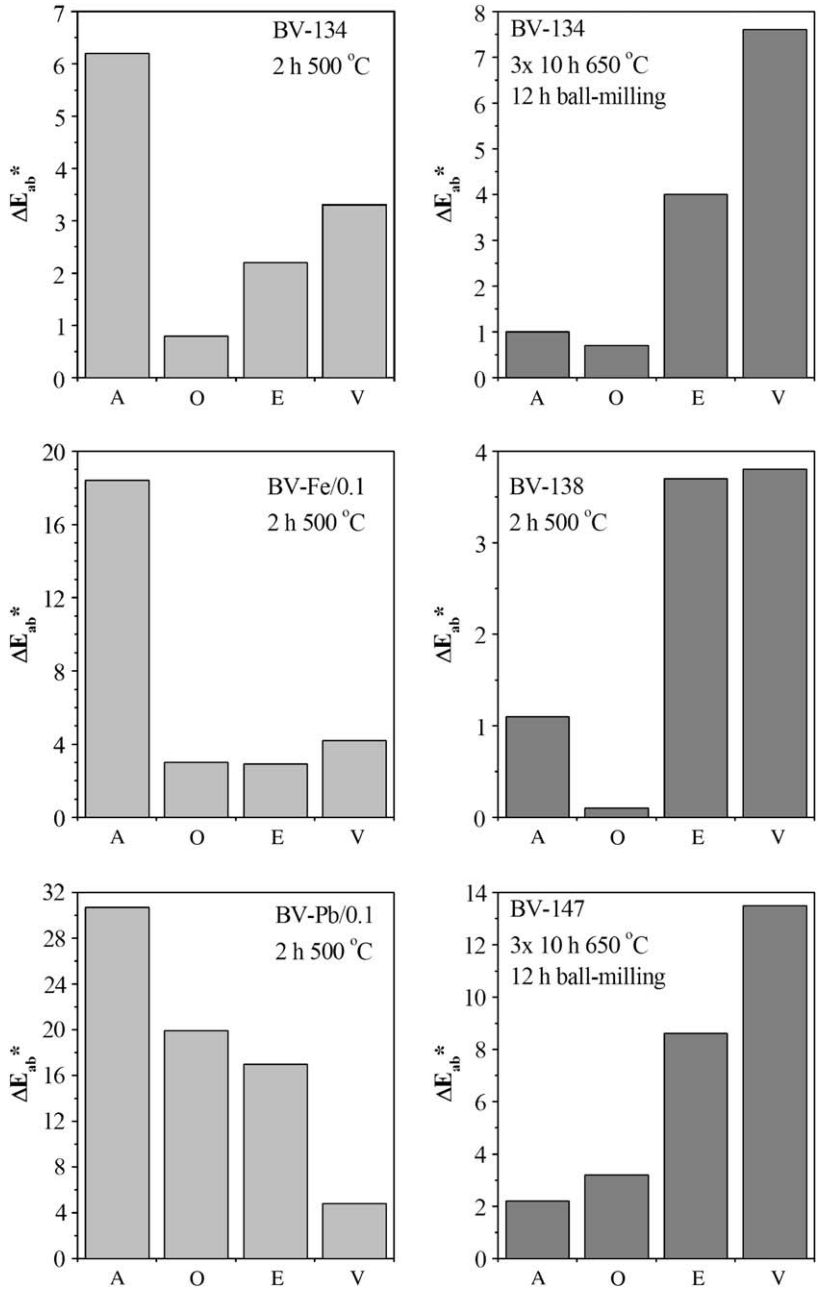

Fig. 5. ΔE_{ab}*-values for illumination of pigment powders in different atmospheres (A = air, O = oxygen, E = air/ethanol, V = vacuum; all samples annealed at 500 °C were thoroughly ground in an agate mortar).

the probability of electron and hole capture by impurities that participate in the PCM. Therefore, shorter lifetimes cause lower ΔE_{ab}*-values. Yamashita [19] studied the influence of oxygen and other gases on the luminescence intensity of photocatalytically active VO_4 or MoO_4 groups bonded to porous SiO_2 substrates. Starting with vacuum, they found considerable drops in intensity after the partial pressure of O_2 was raised, and the presence of adsorbed O_2 quenched the otherwise observed phosphorescence. They also detected the formation of O_2^- after UV irradiation by EPR spectroscopy, and these species turned out to be thermally stable up to approx. 50 °C. Whether similar arguments apply in the case of our findings cannot be taken for granted. The temperatures during illumination fall in a range between about 50 and 60 °C, and the oxygen partial pressure only increases from approx. 0.8 bar (air) to 1.0 bar (pure oxygen). Furthermore, the effect of oxygen on the lifetime of excited states in $BiVO_4$ depends not only on the surface area alone but also on other surface properties (e.g., types of terminating functional groups). More investigations are evidently necessary, but for the time being such an explanation seems to be the most reasonable.

For each pigment sample, a change in PCM should be detectable by a change in the corresponding DRS. Problems will arise if the pigment in question exhibits good lightfastness because low ΔE_{ab}*-values correspond to low DRS intensities. As a consequence of the latter, the characteristic features that are

used to identify the PCM will be less pronounced and, in worse cases, not meaningful at all. The graphs in Fig. 6 show DRS of the samples discussed above. The DRS of BV-138 have been replaced by spectra of several pigment coatings for comparison.

On illuminating the samples BV-134 as well as BV-Fe/0.1 in air, the well-known Fe-type DRS result. According to the surface properties mentioned earlier, the spectra of the former two strongly differ in intensity. When applying reducing atmospheres, the shapes of the DRS change considerably. Whereas the ''double-band feature'' is retained for BV-Fe/0.1 (though intensities drop enormously) after illumination in air/ethanol, the corresponding spectra of BV-134 appear very similar to V-type DRS. Under vacuum conditions, the PCM changes even in the case of BV-Fe/0.1, which now corresponds to BV-147 (pigment coating), and yields a DRS almost identical to that of BV-Pb/0.1. The latter crosses the other spectra of the Pb-doped pigment somewhere between

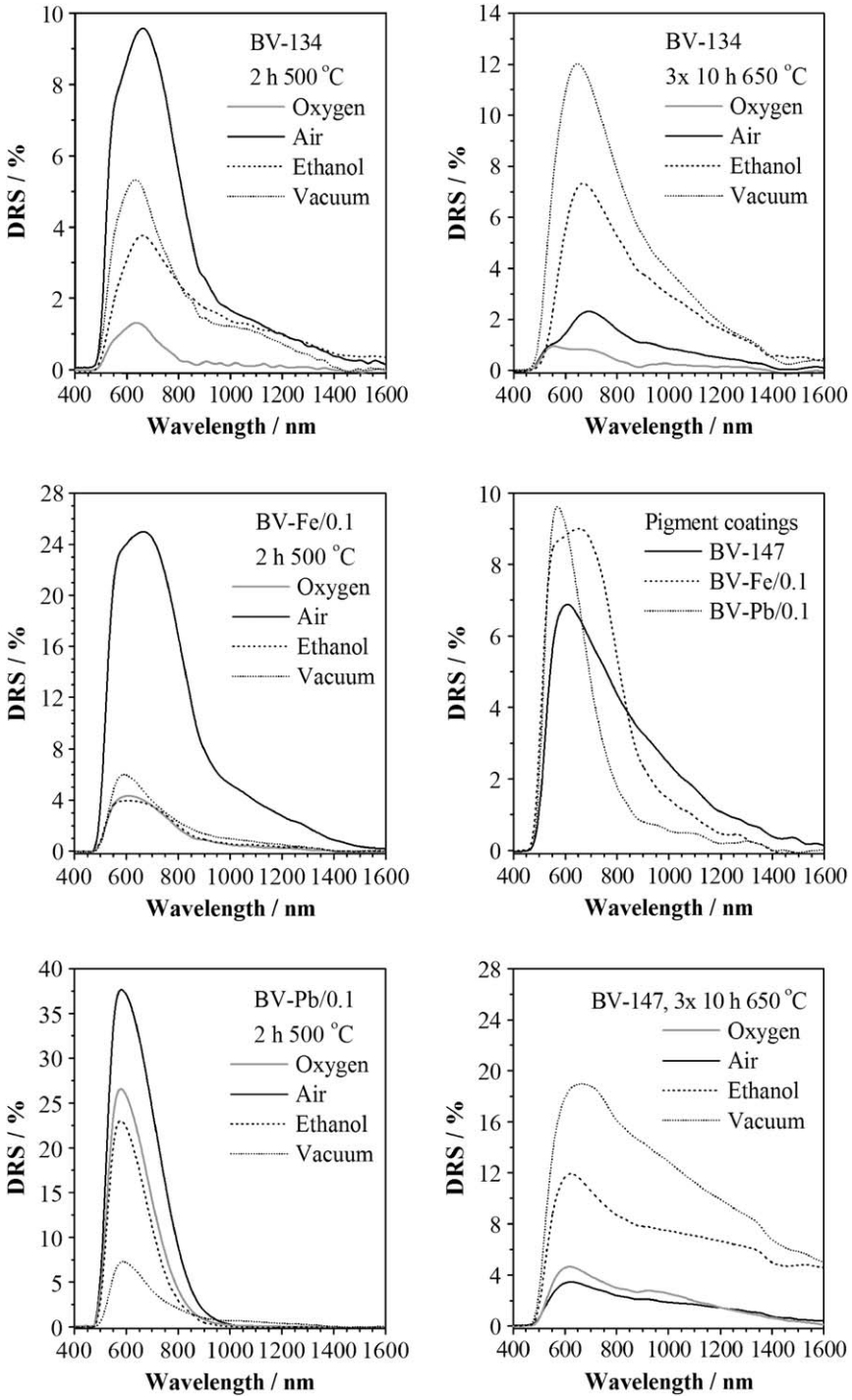

Fig. 6. Difference reflectance spectra (DRS) of powder samples illuminated in different atmospheres.

850 and 1000 nm, and this property, i.e., slowly decreasing intensities, is characteristic for V-type DRS. This kind of mechanism is also relevant to BV-147, where we observe intense DRS after illumination in reducing media. In contrast to what is found for the pigment coating, intensities approach zero only at wavelengths even higher than 1800 nm. To explain this behavior, the formation of V^{IV} defect states, which finally merge into an energy band due to higher defect concentrations, can be taken into account.

Next, we discuss the outcome of reversibility tests for pigment coatings and powders. As implied by the term ''photochromism'', the light induced color change is expected to vanish after keeping the samples in the dark. The time scale can vary depending on the processes involved in the bleaching mechanism. Bechinger et al. [3], who studied the photochromic properties of WO_3 thin films, have found an irreversible contribution to the color change when illuminating in atmospheres free of oxygen. So far we have always assumed that $BiVO_4$ represents a reversible system, but a closer look reveals that this is not always the case. Fig. 7 shows bar charts of ΔE_{ab}*-values calculated from reflectance spectra that were recorded after increasing periods of light exclusion. Basically, we can differentiate three cases. Pigments exhibiting the Fe-type PCM return to their initial state within a few days as is exemplified by BV-Fe/0.1. All Pb-doped compounds need much more time but still appear to be reversible in terms of color change. The third group is made up by pigments that have large surface areas and contain only small amounts of Fe and Pb. In such cases, low ΔE_{ab}*-values result if the samples are kept in air or non-reducing atmospheres during illumination, but there is hardly any decrease in ΔE_{ab}* even after 50 days of light exclusion. The color changes of these samples are difficult to detect visually, but this is no longer the case if vacuum is applied. Fig. 8 shows that for BV-147 $\Delta E_{ab}^* = 5.3$ results after keeping the sample in the dark for 100 days, i.e., we cannot assume complete reversibility.

Finally, we have to address the reversibility of pigment coatings. From the data given in Fig. 8 alone, we must conclude again that the samples do not completely return to their initial states, at least within 70 days. In contrast to these findings, the corresponding reflectance spectra in Fig. 9 suggest a different situation. The dotted curves, which correspond to 70 days of light exclusion, lie slightly above the initial spectra.[4] This can be considered as some kind of ageing, probably due to the rise in temperature during illumination, but does not rule out reversibility in the case of pigment coatings.

3.4. Electron paramagnetic resonance spectroscopy

Irrespective of being reversible or not, changes in color that are not caused by particle size effects imply changes in electronic structure. The latter result from photochemical reactions or photophysical processes that involve one or more species contained in the pigment like, e.g., impurities, dopants or host elements. Additional (metastable) states are created by electron transfer processes and can be detected, under suitable conditions, by electron paramagnetic resonance spectroscopy.

Fig. 10 shows X-band EPR spectra of two powder samples before illumination, namely BV-134 and BV-147. These two examples can serve to illustrate all important spectral features observed for the remaining samples. Both spectra show signals at $g_{\mathrm{eff}} \approx 4.1-4.3$ and 8.6–8.9, which are attributed to high-spin Fe^{III} (see Fig. 12 for comparison), but the signal shapes do not coincide exactly.[5] The Fe signal shown in the left graph might result from more than one Fe species (overlapping of individual signals), or the local structure differs enough to affect the values E and D of the fine-structure tensor $\boldsymbol{D}$.[6,7] At higher magnetic fields we observe characteristic signals of Cu^{II} ($I = 3/2$) and V^{IV} ($I = 7/2$). Depending on the relative amounts of both species, different shapes may result due to signal overlap. Measurements at X-band frequencies cannot resolve the hyperfine lines of ^{63}Cu and ^{65}Cu, but the outermost Cu^{II} hyperfine line at lower magnetic fields is generally well separated from the V^{IV} signal (e.g., see Fig. 13).

Unlike BV-147, the majority of samples contains only small amounts of V^{IV}. In these cases, we often find weak and broad signals without completely resolved hyperfine structure (e.g., see Fig. 14). The spectra in Fig. 10 reveal that the applied thermal treatment (3×10 h 650 °C in air) does not produce larger amounts of V^{IV} by releasing oxygen from the crystal lattice, thereby reducing V^{V} to V^{IV}. Investigations of Shin et al. [20] suggest that, regarding oxygen losses, $BiVO_4$ is thermally more stable than mixtures of Bi_2O_3 and V_2O_5.

We now turn to powder EPR spectra that were recorded before and after illumination in air and reducing atmospheres. Analogous data for pigment coatings are not easily accessible because the properties of the applied baking finish prevent any grinding without chalking, i.e., the separation of pigment particles from the surrounding lacquer. Additionally, broad size distributions as well as electrostatic charging of pigment–lacquer particles make reproducible sample preparation very difficult. Therefore, we have confined our investigations to powder samples only.

Strongly enhanced photochromic effects of BV-134 or BV-Fe/0.1 suggest a vital contribution of Fe to the PCM. We expect photochemically induced oxidation or reduction of Fe^{III}, which is also found in Fe containing perovskites [5,7]. Indeed, powder EPR spectra of both pigments show significantly decreasing intensities of the Fe signal after illumination.

[4] Color differences (ΔE_{ab}*) are usually given as absolute quantities although some information originating from the vectorial properties of color spaces is lost. This fact must be taken into account when analyzing bar charts like those shown in Fig. 8.

[5] We observe "$g = 1/2$ like signals" for compounds that were synthesized by solid-state reaction, but pigments obtained by wet-chemical precipitation give spectra like that of BV-134.

[6] The position of the second maximum in the Fe signal of BV-134 coincides with that of the single maximum of BV-147.

[7] Only in rare cases is it possible to appropriately simulate Fe^{III} signals (like those observed for our samples) on the basis of X-band powder spectra. These difficulties mainly arise from low symmetries, non-coinciding principal axis systems of $\boldsymbol{g}$ and $\boldsymbol{D}$ and the high sensitivity of $\boldsymbol{D}$ to local structure.

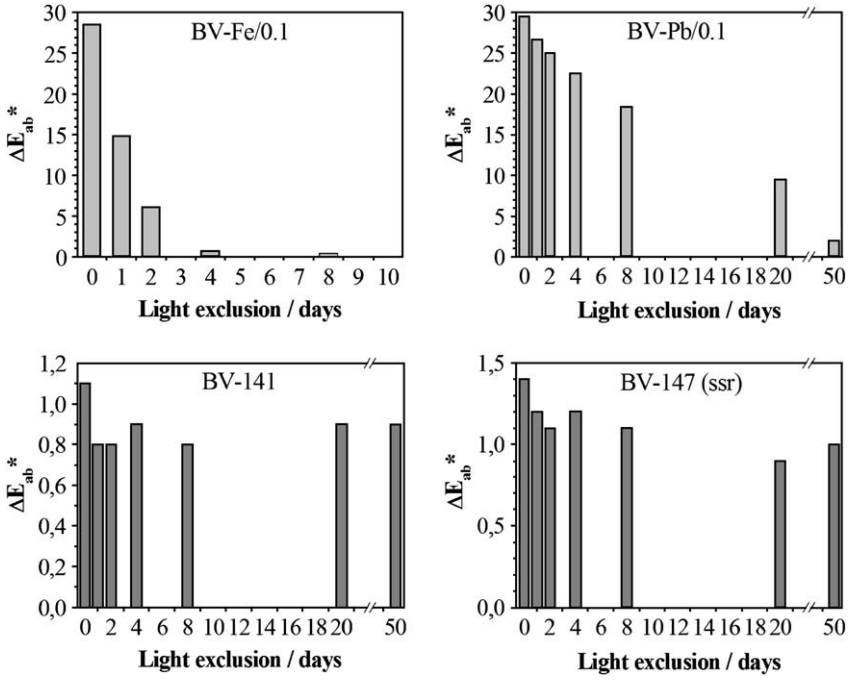

Fig. 7. Reversibility tests for illuminating powder samples in air (BV-Fe/0.1, BV-Pb/0.1: 2 h 500 °C; BV-141, BV-147 (ssr): 3 × 10 h 650 °C, 12 h ball-milling).

On the other hand, no new or enhanced signal appears in the range of 50–450 mT (only the low field region is shown for BV-134). This observation rules out the formation of V^{IV} to compensate for the oxidation of Fe^{III}. We even find slightly decreasing signal intensities for V^{IV} after illumination (BV-Fe/0.1, Fig. 12). In some spectra of compounds with higher Fe levels, another signal of unknown origin occurs at $g_{eff} \approx 2.50$ (Fig. 12, right).

The situation for BV-Pb/0.1 (Fig. 11, right) is somewhat different. In fact, no increase in V^{IV} results as for BV-Fe/0.1, but neither can new paramagnetic centers nor any increase or decrease of existing signals be detected, which could be made responsible for the intense color change of Pb-doped pigments.[8]

To explain these findings, it is important to recognize that, in contrast to Fe^{III}, Fe^{II} as well as Fe^{IV} are spin systems with even total spin quantum number S. In most cases, paramagnetic centers with odd S are easily detectable with standard EPR spectrometers, whereas systems with even S can cause serious problems due to the fine-structure term of the Spin-Hamiltonian. Depending on the local symmetry (***D*** is a traceless tensor), an extended field range is necessary in order to detect the paramagnetic species in question. Therefore, we do not necessarily observe signals of either Fe^{II} or Fe^{IV} within the limited range of 50–450 mT. In fact, only in rare cases has Fe^{IV} ever been identified (e.g., see Ref. [21]). Our results suggest the red-ox disproportionation of Fe^{III} to be the overall process in the Fe-type PCM. This basically simple reaction can involve different steps like, e.g., direct excitation of Fe^{III} or hole-trapping by Fe^{III}. The outcome of illumination experiments in reducing atmospheres is in accordance with the proposed model and supports contributions of oxidized species to the optical properties of illuminated samples (see Fig. 5). The spectra of Pb-doped compounds do not provide as useful information as those of Fe-doped compounds but obviously rule out the formation of Pb^{III}, at least in detectable amounts. Many examples of Pb^{III} spectra are known [22,23], and in all these cases *g*-values between 1.8 and 2.1 have been determined. As Pb^0 and Pb^{IV} are not paramagnetic and V^{III} is an even spin system (for EPR studies of V^{III} in ZnO, where resonance fields at X-band frequencies are found above 450 mT, see Ref. [24]), we cannot gain further insight into the Pb-type PCM on the basis of our EPR studies alone. Situations in which the V-type PCM should be taken into account, i.e., low Fe and Pb concentrations as well as large surface areas, are difficult to analyze, too. Weak photochromic effects correspond to small changes in V^{IV} concentration, which cannot be detected reliably. In this specific case, in-situ illumination of $BiVO_4$ single crystals might be more helpful. Anyway, the V-type mechanism primarily applies to pigment coatings or, generally speaking, to reductive conditions during illumination.

The spectra shown in Figs. 13 and 14 were recorded after illuminating powder samples in either air/ethanol or vacuum. We always observe strong signals of V^{IV}, though for BV-Pb/0.1 illuminated in air/ethanol Cu^{II} dominates the spectrum. In this case, the Cu^{II} signal is a suitable internal standard to compare the V^{IV} concentrations. The graph on the right-hand side of Fig. 13 clearly indicates higher levels of V^{IV} at the time of spectrum recording. Two explanations can be given for this finding. The first accounts for a change in PCM as

[8] The signal at $g_{eff} \approx 2.87$ does not occur in all EPR spectra of intensely photochromic, Pb-doped pigments.

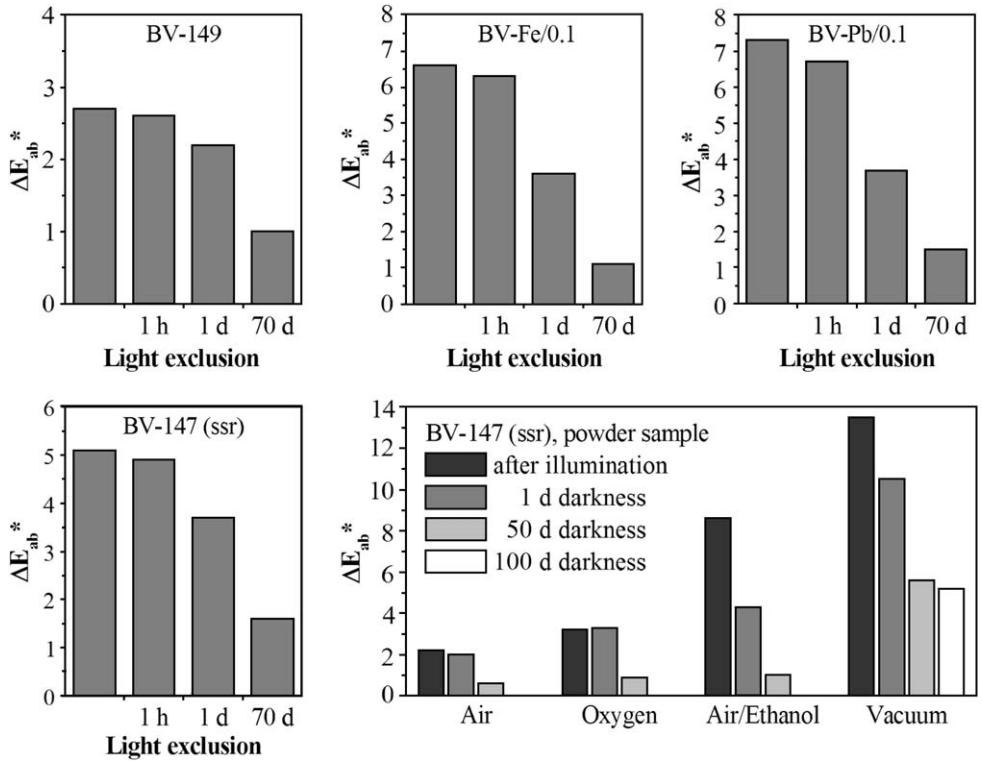

Fig. 8. Reversibility tests for pigment coatings of BV-147, BV-149, BV-Fe/0.1, BV-Pb/0.1 (see text and footnote for explanation), and results for illuminating BV-147 (ssr) in various atmospheres (lower right bar chart).

suggested by the DRS of BV-Pb/0.1 (see Fig. 6). As long as the Pb-type mechanism is operative, only limited amounts of V^{IV} can co-exist with the color determining centers, which are in an oxidized state. This is similar to steady-state situations. Switching to the V-type PCM requires more than only compensation of these centers. Depending on the duration of illumination (kinetics), higher quantities of V^{IV} can be produced. The second explanation involves the differences in reversibility of color change. Even after keeping samples for 100 days in the dark, ΔE_{ab}*-values still as high as 40–50% of the original ones may result for vacuum illumination. The color change of powders that were exposed to air/ethanol declines faster, i.e., the concentration of V^{IV} centers decreases faster. Which explanation applies can only be determined by

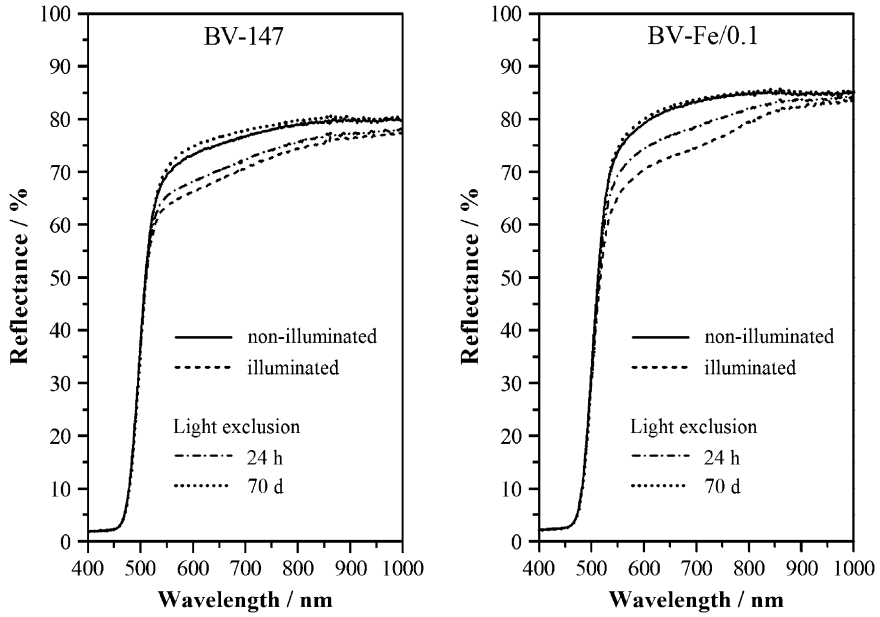

Fig. 9. Diffuse reflectance spectra of illuminated pigment coatings (BV-147, BV-Fe/0.1).

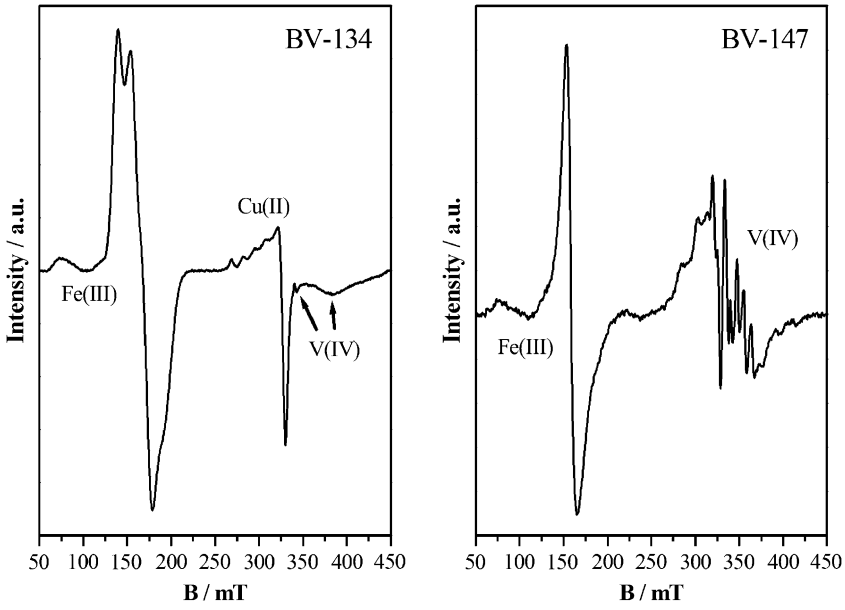

Fig. 10. X-band EPR spectra of BV-134 (3 × 10 h 650 °C) and BV-147 (ssr, 3 × 10 h 650 °C) before illumination.

further studies of the bleaching kinetics, but both agree with the results of our illumination experiments and powder EPR spectroscopy data.

4. Conclusions

Considering the foregoing discussion as well as results of earlier studies [13], we can identify three factors that determine the mechanism and the extent of photochromism for $BiVO_4$ based pigments. The content of two trace impurities, namely Fe and Pb, the specific surface area of the pigment particles and the chemical properties of the surrounding medium affect the color change on light exposure. Our findings suggest three different mechanisms, which we call Fe-type, Pb-type and V-type. As indicated by its name, the first one is operative at higher Fe levels and causes strong photochromic effects. The Fe-type PCM is easily identified on the basis of difference reflectance spectra (DRS) and can be considered to be completely reversible. This applies for powder samples and pigment coatings as well. The most important differences between the Fe-type and Pb-type mechanisms are the periods required to bleach illuminated samples and the shape of the DRS. It is also worth mentioning that the risk of Fe contaminations is substantially higher than that of Pb (under standard industrial production conditions including the choice of educts). In both cases, high ΔE_{ab}*-values result if illumination

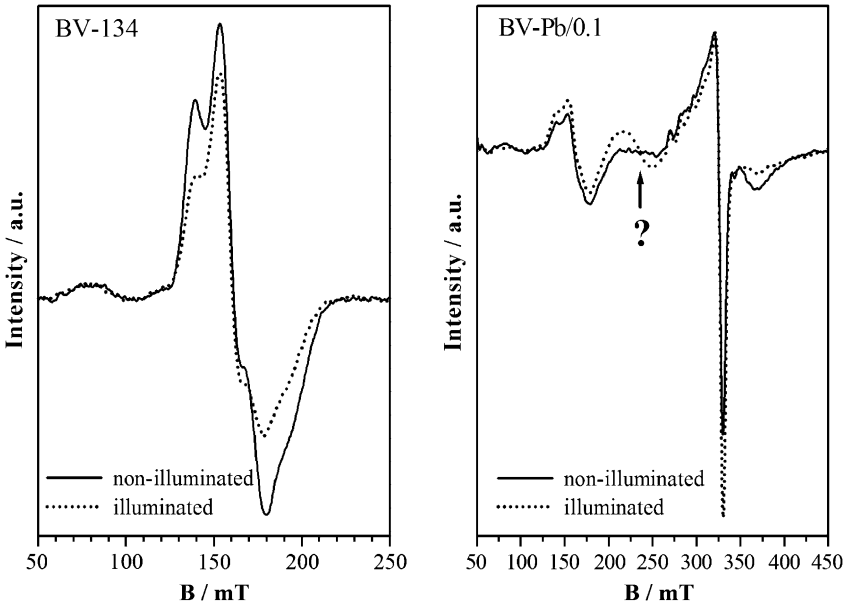

Fig. 11. X-band EPR spectra of BV-134 and BV-Pb/0.1 (2 h 500 °C + 0.5 h 620 °C); illumination in air (dotted graphs).

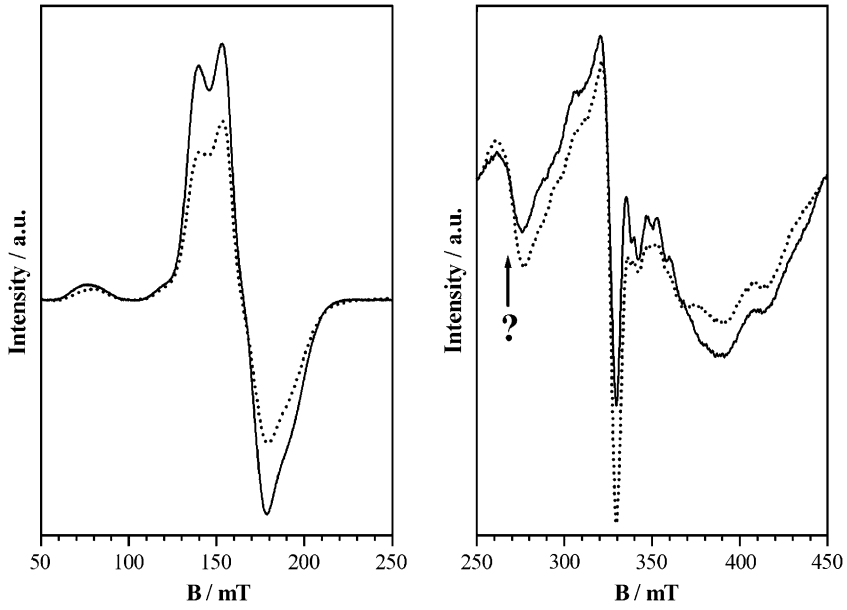

Fig. 12. X-band EPR spectra of BV-Fe/0.1 (2 h 500 °C + 0.5 h 620 °C); illumination in air (dotted graphs) (the spectra on the right have been rescaled for better illustration; intensities in the range from 250 to 450 mT are approx. 100 times lower than the Fe^{III} signal).

of powders is carried out in air and the corresponding samples have small surface areas. Large surface areas or reducing atmospheres, which also include vacuum, cause significant decreases in ΔE_{ab}*. Whereas the former seem to influence the lifetime of excited states due to interactions between pigment particles and their surroundings, the latter involve photochemical reactions with, e.g., hydroxyl groups or liberation of oxygen from the crystal lattice, thereby inhibiting the formation of oxidized species of Fe or Pb. If only small amounts of Fe or Pb are present, the third mechanism (V-type PCM) takes effect, and reducing atmospheres support the formation of V^{IV} centers. Only under such conditions do ΔE_{ab}*-values of 10 and higher result. Depending on the concentration of V^{IV}, defect states or bands appear below the conduction band and give rise to absorption in the visible and far infra-red part of the spectrum. As a result, the single peak DRS decrease more slowly towards longer wavelengths compared to Pb-type spectra. Regarding the outcome of illumination experiments, there is a close resemblance between air/ethanol (powders) and lacquer (pigment coatings), which underlines the reducing properties of the latter. Other impurities might also participate in any of the three PCMs, but so far we have found no indications that their presence is necessarily required (in contrast, compare the PCM of $LiNbO_3$:Fe,Mn [25]).

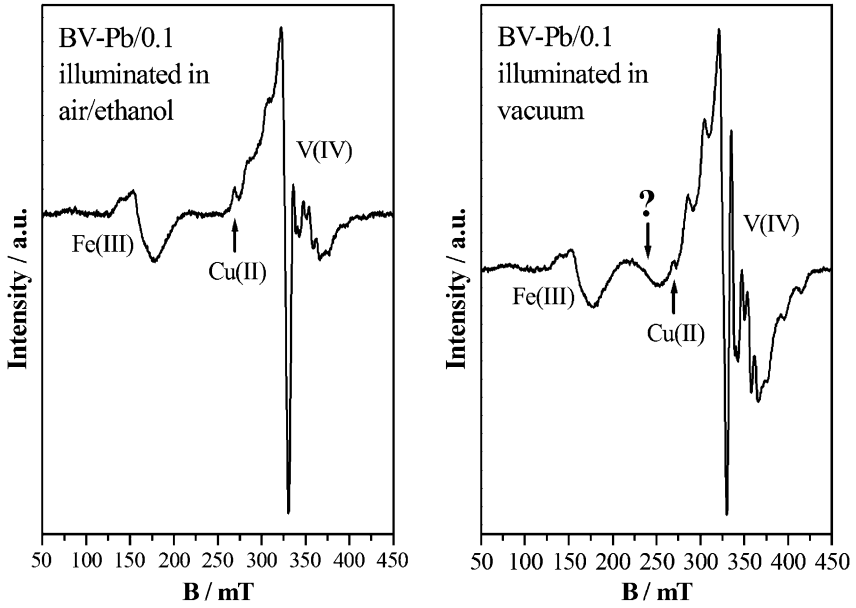

Fig. 13. X-band EPR spectra of BV-Pb/0.1 (2 h 500 °C + 0.5 h 620 °C); illumination in air/ethanol and vacuum.

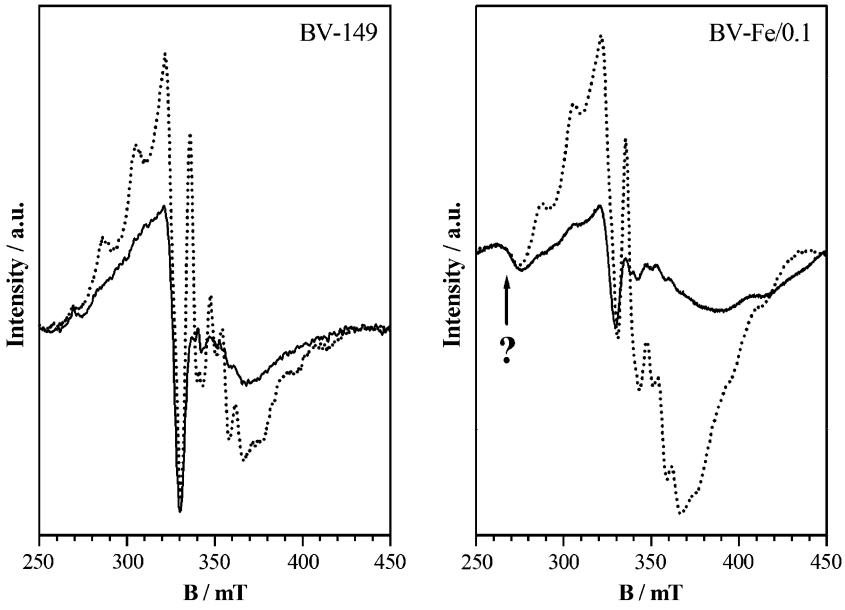

Fig. 14. X-band EPR spectra of BV-149 and BV-Fe/0.1 (2 h 500 °C + 0.5 h 620 °C); illumination in vacuum (dotted graphs).

The V-type PCM can further be subdivided into two groups. Complete reversibility can only be observed for pigment coatings, where the functional groups that take part in photochemical reactions are fixed. On the other hand, illumination in vacuum involves loss of oxygen and creation of oxygen vacancies. The inversion of this process at room temperature (adsorption of oxygen, take-up of electrons, formation and diffusion of oxygen ions into the lattice to refill the vacancies and avoid surface charges) is kinetically unfavorable. Therefore, large color differences remain even after 100 days of light exclusion.

Electron paramagnetic resonance spectroscopy of illuminated powder samples gives deeper insight into the mechanisms and supports some of the ideas that were deduced from illumination experiments. The central step in the Fe-type PCM is the photochemical disproportionation of Fe^{III} to Fe^{II} and Fe^{IV}. There are no indications of increasing V^{IV} levels, i.e., the majority of imaginable red-ox reactions between Fe^{III} and V^{V} can be ruled out. Fe^{IV} seems to be the color determining species because reducing atmospheres largely suppress light induced color changes. For Pb-doped samples, no additional EPR signals (e.g., signals of Pb^{III} or V^{IV}) appear after illumination, but Pb^{0} and Pb^{IV} cannot be detected due to their magnetic properties.

The specific surface area directly affects the extent of interaction between pigment particles and the surrounding medium. Large surface areas and low concentrations of Fe and Pb support the V-type mechanism. The opposite is true for the Fe-type and Pb-type PCM. DRS usually indicate the dominating mechanism, but in some cases, especially for low ΔE_{ab}*-values, results may be ambiguous. There are strong indications that a given Fe (or Pb) concentration "requires" a particular surface area to minimize the photochromic effect. At higher ratios the Fe- or Pb-type mechanism dominates, but at lower ratios the V-type PCM takes effect. This explanation accounts for pigment samples like, e.g., BV-109, BV-138, BV-139, BV-140, whose photochromic properties do not turn out as expected and cannot be understood on the basis of trace analysis alone.

Acknowledgements

We gratefully acknowledge the substantial support of BASF Ludwigshafen and the helpful discussion with Dr. N. Mronga and Dr. O. Seeger. Furthermore, we would like to thank Prof. Dr. J. Hüttermann and Dr. R. Kappl (electron paramagnetic resonance spectroscopy; Institut für Biophysik, Universität des Saarlandes, Germany) as well as Prof. Dr. W. F. Maier (surface measurements; Lehrstuhl für Technische Chemie, Universität des Saarlandes, Germany).

References

[1] Gavrilyuk A. Proc SPIE 1997;2968:195.
[2] Tritthart U, Gavrilyuk A, Gey W. Solid State Commun 1998;105:653.
[3] Bechinger C, Oefinger G, Herminghaus S, Leiderer P. J Appl Phys 1993;74:4527.
[4] Palgrave RG, Parkin IP. J Mater Chem 2004;14:2864.
[5] Huang M-H, Xia J-Y, Xi Y-M, Ding X-X. J Eur Ceram Soc 1997;17:1761.
[6] Koidl P, Blazey KW, Berlinger W, Müller KA. Phys Rev B 1976;14:2703.
[7] Faughnan BW. Phys Rev B 1971;4:3623.
[8] Bochakova TM, Volnyanskii MD, Volnyanskii DM, Shchetinkin VS. Phys Solid State 2003;45:244.
[9] Caurant D, Gourier D, Prassas M. J Appl Phys 1992;71:1081.
[10] Caurant D, Gourier D, Vivien D, Prassas M. J Appl Phys 1993;73:1657.
[11] Stepanov SI. Rep Prog Phys 1994;57:39.

[12] Lee M, Takekawa S, Furukawa Y, Uchida Y, Kitamura K, Hatano H, et al. J Appl Phys 2000;88:4476.
[13] Tücks A, Beck HP. J Solid State Chem 2005;178:1145.
[14] Krill CE, Haberkorn R, Birringer R. Handbook of nanostructured materials and nanotechnology. In: Nalwa HS, editor. Handbook of nanostructured materials and nanotechnology. San Diego: Academic Press; 2000.
[15] http://www.anadat.de; 2000.
[16] Völz HG. Industrial color testing. Fundamentals and techniques. Weinheim: VCH; 1995.
[17] Shannon RD, Prewitt CT. Acta Crystallogr 1975;A32:751.
[18] Yeom TH, Choh SH, Du ML, Jang MS. Phys Rev B 1996;53:3415.
[19] Yamashita H. In: Anpo M, editor. Wiley series in photoscience and photoengineering. Vol. 1: surface photochemistry. Chichester, New York, Brisbane, Toronto, Singapore: John Wiley & Sons; 1996.
[20] Shin MY, Chung KS, Hwang DW, Chung JS, Kim YG, Lee JS. Langmuir 2000;16:1109.
[21] Possenriede E, Jacobs P, Schirmer OF. J Phys: Condens Matter 1992;4:4719.
[22] Pöppl A, Völkel G. Phys Stat Sol 1990;A121:K69.
[23] Seager CH, Warren WL. J Appl Phys 1993;73:7720.
[24] Coffman RE, Himaya MI, Nyeu K. Phys Rev B 1971;4:3250.
[25] Shin H, Ravi G, Uccida Y, Kitamura K, Lee M. Jpn J Appl Phys 2004;Pt. 1(43):7504.